frontiers in Marine Science

ORIGINAL RESEARCH
published: 23 June 2020
doi: 10.3389/fmars.2020.00440

Phylogenetics and Mitogenome Organisation in Black Corals (Anthozoa: Hexacorallia: Antipatharia): An Order-Wide Survey Inferred From Complete Mitochondrial Genomes

Nick J. Barrett[1,2,3]*, *Raissa I. Hogan*[4], *A. Louise Allcock*[4], *Tina Molodtsova*[5], *Kevin Hopkins*[1], *Andrew J. Wheeler*[6] and *Chris Yesson*[1]

[1] Institute of Zoology, Zoological Society of London, Regent's Park, London, United Kingdom, [2] Imperial College London, London, United Kingdom, [3] Natural History Museum, London, United Kingdom, [4] School of Natural Sciences and Ryan Institute, National University of Ireland, Galway, Ireland, [5] P.P. Shirshov Institute of Oceanology, Russian Academy of Sciences, Moscow, Russia, [6] School of Biological, Earth and Environmental Sciences/iCRAG/MaREI/ERI, University College Cork, Cork, Ireland

OPEN ACCESS

Edited by:
Luisa Fernanda Dueñas, National University of Colombia, Colombia

Reviewed by:
Mercer Robert Brugler, New York City College of Technology (CUNY), United States
Jaret Bilewitch, The University of Queensland, Australia

***Correspondence:**
Nick J. Barrett
n.j.barrett@outlook.com

Specialty section:
This article was submitted to Deep-Sea Environments and Ecology, a section of the journal Frontiers in Marine Science

Received: 23 January 2020
Accepted: 19 May 2020
Published: 23 June 2020

Citation:
Barrett NJ, Hogan RI, Allcock AL, Molodtsova T, Hopkins K, Wheeler AJ and Yesson C (2020) Phylogenetics and Mitogenome Organisation in Black Corals (Anthozoa: Hexacorallia: Antipatharia): An Order-Wide Survey Inferred From Complete Mitochondrial Genomes. Front. Mar. Sci. 7:440. doi: 10.3389/fmars.2020.00440

Black corals (Anthozoa: Antipatharia) are an ecologically and culturally important group of deep-sea cnidarians. However, as the majority of species inhabit depths >50 m, they are relatively understudied. The inaccessibility of well-preserved tissue for species of interest has limited the scope of molecular analysis, and as a result only a small number of antipatharian mitochondrial genomes have been published. Using next generation sequencing, 18 complete and five partial antipatharian mitochondrial genomes were assembled, increasing the number of complete mitochondrial genomes to 22. This includes species from six antipatharian families, four of which were previously unrepresented, enabling the first family-level, full mitochondrial gene analysis over the whole order. The circular mitogenomes ranged in size from 17,681 to 21,669 bp with the large range in size due to the addition of an intron in *COX1* in some species and size variation of intergenic regions. All mitogenomes contained the genes standard to all hexacoral mitogenomes (13 protein coding genes, two rRNAs and two tRNAs). The only difference in gene content is the presence of the *COX1* intron in five families. The most variable mitochondrial gene is *ND4* which may have implications for future barcoding studies. Phylogenetic analysis confirms that Leiopathidae is sister to all other families. Families Antipathidae, Cladopathidae and Schizopathidae are polyphyletic, supporting previous studies that call for a taxonomic revision.

Keywords: cnidaria, gene order, next generation sequencing, NGS, HEG, barcoding, deep-sea, COX1 intron

INTRODUCTION

The order Antipatharia Milne Edwards and Haime, 1857, also known as black or thorny corals, is an ecologically and culturally important group of deep-sea anthozoans in the hexacoral subclass (Cnidaria: Anthozoa: Hexacorallia). The order includes 273 species in 45 genera and seven families (Molodtsova and Opresko, 2020), with many new species expected. Black corals are found in every ocean occupying depths from 2–8,600 m (Wagner et al., 2012), but are primarily concentrated at depths >50 m (Cairns, 2007), with ∼50% of known genera inhabiting depths >500 m (Molodtsova and Opresko, 2017). Anipatharians are exclusively colonial and exhibit a diverse range of polyp, skeletal and spine morphologies. They range in height from 5 to 10 cm to >3 m (Wagner et al., 2012). Unlike scleractinian corals, the skeletons of antipatharians are not calcified but are instead rich in protein and chitin [(Bo et al., 2012b); see Ehrlich (2010) for a review] and often appear black when visible. Although not reef forming, antipatharians can play a crucial ecological role in forming coral garden habitats (Bo et al., 2009b) and individuals can support significant epifaunal populations (Love et al., 2007; Roberts et al., 2009). From China to Hawaii, black coral has been utilized in traditional medicine for a wide variety of therapeutic and spiritual uses, while its common use in jewelery has seen commercial harvesting established in the Caribbean, Hawaii and parts of Asia (Wagner et al., 2012). This has resulted in all species of black coral being listed on CITES appendix II. Their use in traditional medicine has led to interest from pharmacologists, with studies showing potential roles in cancer treatments (Qi et al., 2009; Ghandourah and Alorfi, 2019) and the presence of antibacterial properties (Al-Lihaibi et al., 2010).

The use of complete mitochondrial genomes has become an increasingly popular tool for taxonomic and phylogenetic research due to the advances and availability of next generation sequencing technology (Kayal et al., 2013; Crampton-Platt et al., 2016). In addition, metazoan mitogenomes provide a number of genome-level characters that can support phylogenetic hypotheses. These include gene order arrangements, position of introns, insertions and inferred secondary structures of transfer RNAs (tRNA) and ribosomal RNAs (rRNA) (Boore, 2006). In particular, gene order arrangements have proved useful in anthozoan studies by furthering understanding of evolutionary relationships (Brugler and France, 2007; Brockman and McFadden, 2012; Figueroa and Baco, 2014; Hogan et al., 2019) and provided additional resolution when nucleotide and protein sequence phylogenies have proved contradictory (Lin et al., 2014). This is in part due to a number of advantageous features of the mitogenome, including the presence of a near universal homology of mitochondrial genes found across the animal kingdom (Wolstenholme, 1992; Boore and Fuerstenberg, 2008). In addition, the high number of possible gene arrangements suggests that the observed gene order is most likely to be a derived synapomorphy shared among related taxa, rather than the result of a convergent rearrangement (Clayton, 1992; Falkenberg et al., 2007) [however, ancestral state reversions have been observed, see Figueroa and Baco (2014)].

Hexacoral mitogenomes share some unique properties amongst metazoans. Complete mitogenomes have been sequenced for species from each of the five hexacoral orders: Actiniaria (Foox et al., 2015; Zhang et al., 2017), Antipatharia (Brugler and France, 2007; Kayal et al., 2013; Figueroa et al., 2019), Corallimorpharia (Lin et al., 2014), Scleractinia (Medina et al., 2006), and Zoantharia (Sinniger et al., 2007; Chi and Johansen, 2017). Consistent is a reduced set of the 22 tRNAs necessary for mitochondrial translation, with only $tRNA^{-met}$ (Methionine) and $tRNA^{-trp}$ (Tryptophan) being present. In addition, group 1 introns are found within the NADH dehydrogenase subunit 5 gene (*ND5*) with varying numbers of embedded energy pathway genes specific to each order. A second group 1 intron within the cytochrome c oxidase subunit I gene (*COX1*), with an embedded homing endonuclease gene (*HEG*), has also been identified for some species in each of the hexacoral orders (Celis et al., 2017).

The first sequenced antipatharian mitochondrial genome, *Chrysopathes formosa* was circular and contained 13 energy pathway genes, two ribosomal RNA genes and a reduced number of tRNA genes consistent with all hexacorals (Medina et al., 2006; Brugler and France, 2007; Lin et al., 2014; Foox et al., 2015; Chi and Johansen, 2017). The gene order was described as most similar to the sea anemone *Metridium senile*, with the exception of a transposition of three continuous genes *COX2-ND4-ND6* and lack of a *COX1* intron. However, the subsequent fully sequenced antipatharian mitogenomes, *Stichopathes luetkeni* (Kayal et al., 2013), *Myriopathes japonica* (GenBank NC_027667.1), *Tanacetipathes thamnea* (Figueroa et al., 2019) and the partially sequenced *Leiopathes glaberrima* (Sinniger and Pawloski, 2009) had a *COX1* intron containing a *HEG* gene. With the exception of the *COX1* intron, gene content was the same as in *C. formosa*. The *ND5* intron contains two embedded genes; the only copies of *ND1* and *ND3*, as in actiniarians (Foox et al., 2015; Zhang et al., 2017) and zoantharians (Sinniger et al., 2007; Chi and Johansen, 2017).

Molecular approaches to examining phylogenetic relationships within Antipatharia are a relatively recent addition to systematic studies (Lapian et al., 2007; Wagner et al., 2010; Bo et al., 2012a). Nuclear ribosomal genes (rRNA) and their associated internal transcribed spacers (*ITS1* and *ITS2*) have been effective in resolving phylogenetic relationships within Antipatharia (Lapian et al., 2007; Lapian, 2009; Bo et al., 2012a, 2018). Mitochondrial DNA has been used in a number of antipatharian phylogenetic studies in addition to nuclear DNA, focusing on intergenic regions (IGRs) spanning trnW-*ND2* and *COX3-COX1* (Wagner et al., 2010; Brugler et al., 2013; MacIsaac et al., 2013) and also *ND5-ND1* (Brugler et al., 2013; MacIsaac et al., 2013). Most studies have focused on clarifying the relationships within or between the families Antipathidae, Aphanipathidae, and Myriopathidae (Lapian et al., 2007; Bo et al., 2009a, 2012a; Lapian, 2009; Wagner et al., 2010), while MacIsaac et al. (2013) was the first to examine relationships within Schizopathidae. To date, only one molecular study has included species from all seven antipatharian families, providing the first full family phylogeny (Brugler et al., 2013). However, the

regions examined in that study were unable to fully resolve the phylogeny, particularly at basal nodes.

This study aims to expand our knowledge of antipatharians through sequencing and examining complete mitochondrial genomes from species representing six families. Previously sequenced antipatharian mitogenomes downloaded from GenBank are re-analyzed alongside those from this study, expanding the analysis to cover all seven families.

MATERIALS AND METHODS

Sampling and DNA Extraction

Antipatharian coral samples were collected from surveys around Whittard Canyon, north of the Porcupine Bank and adjacent to the Belgica Mound Province SAC in the NE Atlantic (Irish Margin) at depths of 669–2,817 m, between 2013 and 2017 using a remotely operated vehicle (ROV) *Holland I* onboard the R/V *Celtic Explorer*. Species identifications were made by examining morphological traits based on *in situ* and *ex situ* photographs with reference to classic and current taxonomical literature. Whole genomic DNA was extracted from tissue using the NucleoSpinVR^{TM} tissue Kit (Macherey-Nagel, Düren, Germany) following manufacturer's instructions.

Sequencing Preparation

Samples were prepared for sequencing following the TruSeq DNA PCR-Free Library Preparation Kit protocol (Illumina Inc., San Diego, CA), with the exception of *Tylopathes* n. sp. which was prepared following the QIAseq FX DNA Library protocol (QIAGEN). For the TrueSeq samples DNA was fragmented to a target insert size of 550 bp using a Covaris Focused-ultrasonicator M220^{TM}. Twenty-three samples were sequenced on a single run of an Illumina MiSeq (MiSeq Reagent Kit v3 600-cycle).

Clean up and Assembly

Read quality was assessed using FastQC (Andrews, 2010). Illumina TruSeq index adapters were trimmed and low quality reads (Q<28) removed using cutadapt 2.3 (Martin, 2011). Mitogenome assembly was carried out *de novo* in MITObim 1.9.1 (Hahn et al., 2013) utilizing the *COX1* seed sequence from *Chrysopathes formosa* (GenBank accession number: NC_008411.1). Complete circular read coverage was confirmed by mapping the clean reads onto the assembled circular sequence in Geneious Prime 2019.2.1 (Kearse et al., 2012) (see **Supplementary Material** for additional detail).

Genome Annotation

Protein coding regions, tRNAs and rRNAs were identified in Geneious using the live annotate function based on three published antipatharian mitogenomes (GenBank accession numbers: *Chrysopathes formosa* NC_008411.1, *Stichopathes luetkeni* JX023266.1, *Myriopathes japonica* NC_027667.1). Additionally, confirmation was sought using the online tool Mitos2 (Bernt et al., 2013) with NCBI RefSeq 81 Metazoa and genetic code 4 (mold, protozoan and coelenterate mitochondrial code). Annotations were manually edited using the widest possible open reading frame for protein coding regions based on genetic code 4 and cnidarian start (ATG) and stop (TAG, TAA) codons. Intron boundaries were confirmed manually using homologous regions in non-intron containing taxa. The position of tRNAs were confirmed using tRNAscan-SE (Lowe and Chan, 2016).

Genome Composition

Nucleotide composition and GC content were calculated in Geneious. Relative GC and AT skew was calculated using the skew formula of Perna and Kocher (1995). Origins of replication were predicted using the DNA walker method (Lobry, 1996) within GraphDNA (Thomas et al., 2007) which assesses for abrupt switches in polarity in the asymmetry of strand specific frequencies of nucleotide composition. All genomes were assessed for tandem repeats using Tandem Repeats Finder (Benson, 1999) and inverted repeats using EMBOSS einverted (Rice et al., 2000).

Nuclear DNA

Nuclear ribosomal DNA spanning the region partial 18S rRNA, *ITS1*, 5.8S rRNA, *ITS2* and partial 28S rRNA were assembled from the cleaned reads using a combination of MITObim (see above) and read mapping onto a reference sequence (*Chrysopathes formosa*, GenBank accession number MG023168.1).

Alignment for Phylogenetic Analysis

The 13 mitochondrial protein coding genes and five nuclear regions were aligned separately in MAFFT v7.407 (Katoh and Standley, 2013) using the L-INS-i method; maxiterate: 1000, as this showed the highest pairwise identity (PI) and percentage of identical sites (IS). Each alignment was processed through Gblocks 0.91b (Castresana, 2000) which improves alignments for phylogenetic analysis by removing poorly aligned and divergent regions (see **Table S1** in **Supplementary Material** for Gblock parameters). Concatenated sequences were created for (a) the 13 mitochondrial genes; (b) five nuclear regions; and (c) combined mitochondrial and nuclear regions, using a seqCAT.pl (Bininda-Emonds, 2005) script. Published genomes used in this study were re-analyzed alongside the newly sequenced genomes.

Phylogenetic Analysis

Three phylogenies were constructed from the concatenated sequences; (a) the 13 mitochondrial genes (30 taxa; 12,227 characters); (b) five nuclear regions (29 taxa; 10,28 characters); (c) combined mitochondrial and nuclear regions (29 taxa; 13,255 characters), using maximum likelihood (ML) implemented in IQ tree (Nguyen et al., 2014) and Bayesian inference (BI) statistics implemented in MrBayes 3.2.6 (Ronquist et al., 2012). Due to the lack of a suitable nuclear sequence, *Stichopathes luetkeni* and *Tanacetipathes thamnea* were left out of the nuclear dataset phylogeny. As nuclear regions for *Myriopathes japonica* were unavailable, the congeneric *Myriopathes myriophylla* (GenBank accession number AM404328.1) was used to create a chimeric sequence for *Myriopathes* in the combined dataset phylogeny, and as the single representative of *Myriopathes* in the nuclear phylogenies. *Edwardsia timida* replaced *Nematostella* sp. within

the outgroup of the nuclear phylogeny, as suitable nuclear sequences were unavailable for *Nematostella* sp.. A chimeric sequence consisting of nuclear regions for *E. timida* and 13 mitochondrial genes of *Nematostella* sp. represented the family Edwardsiidae as an actiniarian outgroup in the combined phylogeny. Models of sequence evolution were determined for each Gblock-edited region using jModelTest 2.1.10 (Guindon and Gascuel, 2003; Darriba et al., 2012) based on AIC scores, and implemented in Bayesian analysis (see **Table S2** for models). Partitions for each region were also input to IQtree which runs an automatic model testing and selection using ModelFinder (Kalyaanamoorthy et al., 2017) (**Table S2**). Both IQtree and MrBayes analyses were carried out on the CIPRES Science Gateway V. 3.3 (Miller et al., 2010). For ML analysis, 1,000 bootstrap replicates were performed within IQtree using the ultrafast bootstrap (Hoang et al., 2017). Bayesian analysis ran for 10 million generations, sampling every 1000 generations on two separate runs and four chains. All runs were visualized in Tracer v1.7.1 (Rambaut et al., 2018). All runs showed an effective sample size >6,000. A burn-in of 1 million was applied and a single target tree obtained using TreeAnnotator v1.10.4 (Bouckaert et al., 2014). Tests of monophyly were performed by running constrained analyses fixing the monophyly of selected groups and comparing likelihoods with the unconstrained tree using an approximately unbiased (AU) test (Shimodaira, 2002).

Outgroup Selection

We have included a representative from each of the four additional hexacoral orders, including three from Actiniaria as outgroups. Phylogenies are rooted at a midpoint between Antipatharia and the hexacoral outgoups to examine Antipatharia monophyly rather than examine hexacoral relationships. (see **Table S3** for GenBank accession numbers). Phylogenies with different outgroup combinations were explored to assess ingroup topology consistency (see **Figures S1–S3**).

RESULTS

Genome Organisation

Eighteen complete and five partial mitochondrial genomes of 23 deep-sea antipatharian morphospecies from the Northeast Atlantic, were assembled and annotated (**Table 1**). These represent 14 genera and six families. The 18 complete genomes are circular and range in size from 17,679 (*Tylopathes* n. sp.) to 21,669 bp (*Leiopathes* cf. *glaberrima*) with the size range primarily due to the addition of the *COX1* intron and size variation of IGRs. Partial mitogenomes were recovered for five morphospecies. Two of these were almost complete, with *Leiopathes montana* missing a 156 bp gap (predicted based on genome similarity to *L.* cf. *glaberrima)* and *Antipathes* cf. *dichotoma* missing a 9 bp gap (predicted based on genome similarities to the three additional Antipathidae samples) and possessing 16 ambiguous sites. Three samples (*Chrysopathes* cf. *micracantha*; *Cladopathes* cf. *plumosa*; *Trissopathes grasshoffi*) yielded very limited coverage, resulting in the recovery of 3.2, 48.2, 1.9%, respectively, of a full-size genome (based on the full genome size of *Trissopathes* cf. *tetracrada* and *Chrysopathes formosa).*

All recovered genomes contain 13 energy pathway genes (*COX1-3, ND1-6, ND4L, CYTB, ATP6,* and *ATP8*), two tRNAs ($tRNA^{-met}$ and $tRNA^{-trp}$) and two subunit rRNAs (12S and 16S) (**Table 2**). Genomes from eight samples are interrupted by a group 1 intron in *COX1* at the same insertion site, the ‘3 end of position 884 [see Emblem et al. (2011) for intron nomenclature]. Additionally, all taxa with *COX1* introns contain a *HEG* gene which varies in length from 657 (*Myriopathes japonica, Tanacetipathes thamnea* and *Tylopathes* n. sp.) to 1,062 bp (*Stichopathes luetkeni*). All genomes contain a group 1 intron in *ND5* with the same insertion site at the ‘3 end of position 717, containing the only genome-wide copies of *ND1* and *ND3*. All genes are separated by IGRs which show large size variation (**Table 2**; see **Table S4** for full species table).

Across all samples the largest IGR is found between *ND4* and *ND6* in *Phanopathes* sp. and extends for 597 bp. However, the range for this region between samples is 531 bp, extending for only 66 bp in *C. formosa.* The smallest IGR is found between *ND6* and *ATP8* in *M. japonica, T. thamnea* and *Tylopathes* n. sp. and extends for 4 bp. The genomes with the largest total intergenic space are *L.* cf. *glaberrima* and *L. montana* both with a length of 2912 bp, while *M. japonica* has the smallest at 716 bp.

A number of novel ORFs were identified within the IGRs (see **Table S5**) The largest ORF is found exclusively in *Phanopathes* sp. in the IGR *ND4-ND6* spanning 477 bp. No single ORF was found consistently across all samples, however within families there are conserved ORFs of the same length and at the same location.

Gene content within the sample genomes shows two variations (**Figure 1**), with the only variation due to the absence of the *HEG* gene in the families Schizopathidae and Cladopathidae. All genes are transcribed in the same direction and on the same strand.

Analysis of Base Composition

Whole genome base composition is A+T rich ranging from 64.8 (*Stichopathes luetkeni*) to 58.3% (*Antipathes* cf. *dichotoma* and *Stichopathes abyssicola*) (**Table 3**). GC skew was positive ranging from 0.084 (*Tylopathes* n. sp.) to 0.129 (*Stichopathes luetkeni*), while AT skew was negative ranging from −0.116 (*Myriopathes japonica*) to −0.097 (*Leiopathes montana*).

The DNA walk method found four abrupt changes in base composition across all genomes (**Figure 2**). These are found in the intergenic regions *ND2*-12S, 12S-*CYTB, trnM*-16S and 16S-*COX3*. An additional reversal in polarity is present only in samples with the *COX1* intron, marking the boundaries of the intron. These junctions suggest the genome is split into four blocks (**Figure 1**); block 1: *COX3-ND2*, block 2: 12S, block 3: *CYTB-trnM*, block 4: 16S, and an additional block for samples with the *COX1* intron; block 5: *COX1* intron. Three of the IGR which show abrupt changes in polarity are rich in A+T content across all genomes; *ND2*-12S A+T range of 60.5 to 70.5%, *trnM*-16S A+T range of 58.4 to 71.4% and 16S-*COX3* A+T range of 56.4 to 69.4% (data not shown). The only tandem repeats (>15 bp) were a 37 bp sequence found in the IGR *COX2-ND4* in two samples *S. abyssicola* and *A.* cf. *dichotoma*, and a 22 bp repeat found in *M. japonica* within the *COX1* intron. Inverted repeats

TABLE 1 | Antipatharian samples, GenBank accession numbers, collection information and sequencing data used in this study.

Family	Species	Depth (m)	Location	Reads	Cleaned reads	Mt reads	MtDNA (bp)	Mean coverage (mitogenome)	Min-Max coverage (mitogenome)	Mitogenome genbank number	Nuclear region genbank number
Antipathidae	*Antipathes* cf. *dichotoma*	699	Whittard canyon	1,685,538	585,418	566	19,944	6.6	0–16	MT318841	MT318863
Antipathidae	*Stichopathes abyssicola*	2,037	Whittard canyon	496,172	421,188	1,021	19,968	13	2–25	MT318856	MT318880
Antipathidae	*Stichopathes* n. sp.	2,032	Whittard canyon	2,630,734	907,933	2,322	19,839	28.8	9–50	MT318857	MT318881
Aphanipathidae	*Phanopathes* sp.	1,197	North porcupine bank	1,052,876	973,699	1,863	20,304	24	10–47	MT318852	MT318876
Cladopathidae	*Chrysopathes* cf. *micracantha*	1,113	Whittard canyon	235,548	39,152	166	599	n/a	0	MT318860	MT318867
Cladopathidae	*Cladopathes* cf. *plumosa*	2,049	Whittard canyon	101,256	61,631	55	8,892	n/a	0	MT318861	MT318868
Cladopathidae	*Sibopathes* cf. *macrospina*	9,40	North of belgica mound province SAC	901,890	863,023	992	17,734	15	3–30	MT318853	MT318877
Cladopathidae	*Trissopathes grasshoffi*	1,157	Whittard canyon	36,046	6,815	82	346	n/a	0	MT318862	MT318884
Cladopathidae	*Trissopathes* cf. *tetracrada*	1,853	Whittard canyon	1,432,998	1282,414	3,550	18,469	51.3	24–78	MT318840	MT318883
Leiopathidae	*Leiopathes expansa*	1,113	Whittard canyon	1,105,940	534,005	1,268	21,653	14.4	5–27	MT318847	MT318871
Leiopathidae	*Leiopathes* cf. *glaberrima*	1,836	Whittard canyon	1,826,652	473,685	963	21,669	8.3	1–19	MT318846	MT318870
Leiopathidae	*Leiopathes montana*	669	East of Hovland Mound Province SAC	803,208	266,270	601	21,516	4.9	0–13	MT318848	MT318872
Schizopathidae	*Bathypathes* sp. 1	1,062	Whittard canyon	1,328,558	1222,789	2,037	17,700	30.6	12–52	MT318844	MT318866
Schizopathidae	*Bathypathes* n. sp. 2	2,580	Whittard canyon	461,654	437,111	703	17,700	11	1–24	MT318842	MT318864
Schizopathidae	*Bathypathes* n. sp. 3	2,817	Whittard canyon	1,069,638	800,519	975	17,700	14	4–26	MT318843	MT318865
Schizopathidae	*Dendrobathypathes* n. sp.	1,128	whittard canyon	482,390	461,590	1009	17,687	14	1–28	MT318845	MT318869
Schizopathidae	*Parantipathes* sp.	1,385	Porcupine bank	1,037,636	709,210	519	17,734	7.8	1–16	MT318851	MT318874
Schizopathidae	*Parantipathes hirondelle*	1,014	North porcupine bank	699,038	672,868	643	17,734	9.4	2–21	MT318850	MT318875
Schizopathidae	*Parantipathes* cf. *hirondelle*	1,872	Whittard canyon	2,568,388	208,3001	1,436	17,734	21.2	7–36	MT318849	MT318873
Schizopathidae	*Stauropathes arctica*	1,446	North porcupine bank	904,642	876,101	1,718	17,700	26	12–45	MT318854	MT318879
Schizopathidae	*Stauropathes* cf. *punctata*	1,397	North porcupine bank	1,058,472	987,673	2,456	17,690	37	22–58	MT318855	MT318878
Schizopathidae	*Telopathes* sp.	1,830	Whittard canyon	2,574,466	1,891,358	4,417	17,681	65.3	39–96	MT318858	MT318882
Stylopathidae	*Tylopathes* n. sp.	918	Whittard canyon	1,041,992	9,29,107	2,353	17,679	19.8	4–48	MT318859	MT318885

TABLE 2 | Antipatharian family gene lengths (bp), intergenic regions (italicized) (bp), intron regions (bold) (bp) and gene variation from Gblock alignments (percentage identical sites and percentage pairwise identity).

	Antipathidae	Aphanipathidae	Cladopathidae	Leiopathidae	Myriopathidae	Schizopathidae	Stylopathidae	Identical Sites %	Pairwise Identity %
COX1	1,593–1,629	1,593	1,590–1,629	1,593	1,581	1,590	1,581	75.6	92.8
COX1(5′)-HEG	272–373	344		378	184–206		184		
HEG	981–1,062	981		996	657		657		
HEG-COX(3′)	91–105	103		213	61		61		
COX1-ND4L	35–148	106	92–138	169	83	92	83		
ND4L	300	300	300	300	300	300	300	76.7	93.9
ND4L-COX2	107–340	134	82–128	157	30	70–82	30		
COX2	750	750	750	750	750	750	750	72.3	92.2
COX2-ND4	56–98	82	60–61	110	10	60–61	10		
ND4	1,476	1,476	1,476	1,476	1,476	1,476	1,476	70.5	91.9
ND4-ND6	121–205	597	66–121	174	77	104–112	77		
ND6	579–591	579	564–633	579	570	564	570	70.2	92.0
ND6-ATP8	61–114	113	24–61	64	4	21–24	4		
ATP8	213	213	213	213	213	213–216	213	70.5	93.3
ATP8-ATP6	19–156	19	82–92	233	9	72–82	9		
ATP6	699–720	699	699–714	699	699	699	699	75.4	93.3
ATP6-ND5	28–175	116	108–175	186	25	65–110	25		
ND5	1,851–1,962	1,866	1,839–1,851	1,851	1,851	1,839	1,851	73.1	92.5
ND5(5′)-ND1	350–453	441	367–407	572	253	355–367	253		
ND1	984–1,050	984	984	984	984	984	984	75.5	93.6
ND1-ND3	12–137	109	48	49	5	32–48	5		
ND3	357	357	357	408	360	357	360	75.1	93.3
ND3-ND5(3′)	106–168	106	115–136	221	97	115	97		
ND5-trnW	38–44	39	27–39	39	33	27	33		
trnW	70	70	70	70	70	70	70		
trnW-ND2	19–119	81	19	518–534	17	19	17		
ND2	1,518–1,575	1,575	1,518–1,575	1,584–1,587	1,488	1,509–1,518	1,488	70	91.4
ND2-12S	229–277	258	197–238	431	120	197	154		
12S	1,139–1,170	1,171	1,141–1,168	1,164	1,148	1,141	1,089		
12S -CYTB	69–122	61	100–122	106	65	71–110	66		
CYTB	1,143	1,143	1,143	1,143	1,137	1,134–1,143	1,137	72.7	92.5
CYTB-trnM	51–76	39	49–75	68	59	49	59		
trnM	71	71	71	71	71	71	71		
trnM-16S	66–104	141	64–83	202	48	64–74	42		
16S	2,588–2,663	2,662	2,569–2,588	2,673	2,255–2,256	2,560–2,590	2,252		
16S-COX3	154–224	57	96–224	277	101	74–155	101		
COX3	789	789	750–789	819	789	789	789	73.1	92.7
COX3-COX1	44–296	79	34–69	113	30	34	30		
Total IGR (bp)	1,486–2,160	2,031	1,187–1,686	2,896–2,912	716–717	1,122–1,203	745		

*Blank cells in Cladopathidae and Schizopathidae columns are due to the lack of the COX1 intron. Note that total IGR does not include intron regions. See **Table S4** for full species table.*

(>15 bp) were found in six samples (**Table S6**), with the only consistent repeats being found in the three *Leiopathes* samples.

Protein Coding Genes and rRNAs

Protein coding gene length was similar across all genomes (**Table 2**), with *ND5* varying most in length, while the lengths of *COX2* and *ND4L* were conserved across all antipatharians. The *ND4L* gene varied least (93.9% PI; 76.7% IS) while *ND2* varied most with 91.4% PI and 70% IS, however the variation is due to multiple indels. The most variable gene free of indels was *ND4* (91.6% PI; 70.4% IS). The large ribosomal subunit 16S varied widely in length across species and was the largest assigned region of the genome.

Phylogenies

Phylogenetic analyses (mitochondrial, nuclear and combined) produced largely congruent trees (**Figure 3**; see **Figures S4–S7** for nuclear regions and combined trees). Various combinations

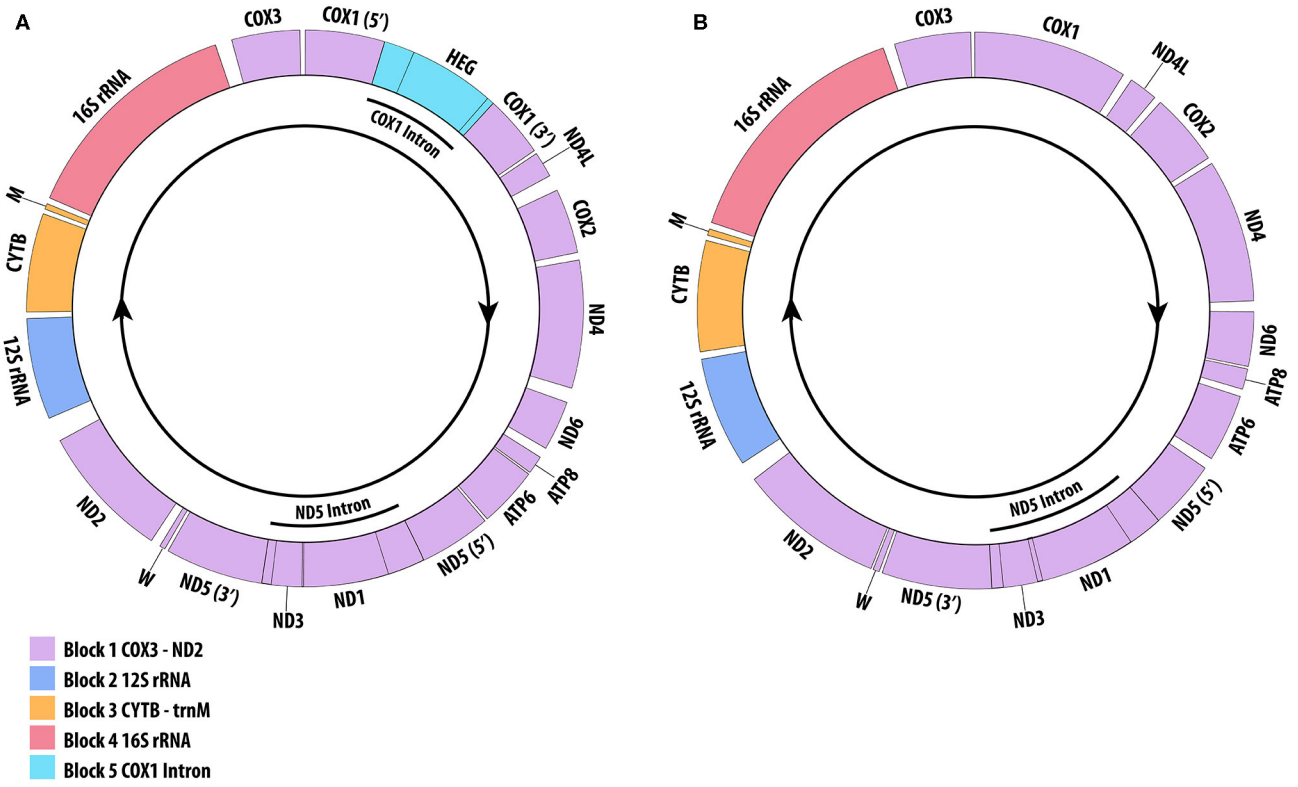

FIGURE 1 | Antipatharian mitogenome graphical map showing gene blocks and gene orders. tRNAs are displayed according to their one letter code. **(A)** Representative of families Antipathidae, Aphanipathidae, Leiopathidae, Myriopathidae and Stylopathidae with the *COX1* intron (relative size based on *Stichopathes abyssicola*). **(B)** Representative of families Cladopathidae and Schizopathidae with the absence of the *COX1* intron (relative size based on *Stauropathes* cf. *punctata*). Arrow indicates direction of transcription. Gene map created using OGDraw (Greiner et al., 2019).

of hexacoral outgroups (see **Figures S1–S3**) confirm the monophyly of Antipatharia and maintain the same ingroup topology. The family Leiopathidae formed a monophyletic group sister to all other antipatharians. The families Antipathidae (in the mitochondrial and combined phylogenies only), Cladopathidae and Schizopathidae (due to the placement of *Sibopathes* cf. *macrospina* nesting within a clade containing three *Parantipathes* spp) did not form monophyletic groups. The genera *Bathypathes, Parantipathes*, *Stauropathes, Stichopathes* and *Trissopathes* did not form monophyletic groups. Constraining the monophyly of each polyphyletic group produced a significantly worse likelihood value tree compared to the unconstrained tree ($P < 0.005$; see **Figure S8**).

DISCUSSION

This study increases the total number of complete antipatharian mitochondrial genomes represented in the literature from four to 22, with five additional partial sequences. This includes species from four families previously unrepresented, enabling for the first time, a family-level full mitochondrial gene analysis over the whole order.

Genome Organization, Gene Order, and Variable Regions

Based on our analysis, antipatharian mitogenomes have the same features typical of all published hexacoral order mitogenomes (Lin et al., 2014; Chi and Johansen, 2017; Zhang et al., 2017). Gene order and content are highly conserved across the antipatharian order, consistent with previous findings (Brugler and France, 2007; Kayal et al., 2013) with the absence of the *COX1* intron as the main notable variation. Internal gene rearrangements have been reported within all hexacoral orders (Emblem et al., 2011; Lin et al., 2014; Foox et al., 2015), but it appears that antipatharians are an exception, along with zoantharians (Poliseno et al., 2020). The stable structural arrangement in these two orders may be linked to the slow rate of nucleotide substitution in anthozoans (Hellberg, 2006).

Metazoan mitochondrial DNA, and specifically *COX1*, was originally viewed as an attractive target for barcoding as it was thought to be almost entirely free of introns and showed a greater range of diversity than other mitochondrial genes (Hebert et al., 2003). In the present analysis, *COX1* has more identical sites and a higher PI (92.8% PI; 75.6% IS), than seven other mitochondrial genes (see **Table 2**). *ND2* varies most (91.4% PI; 70% IS), however, the presence of indels, ranging from 6 to 20 bp at multiple locations, drives this variability. The highest variability seen in an

TABLE 3 | Antipatharian mitochondrial genome nucleotide compositions (from this study and GenBank species).

Species	Total bp	A	C	G	T	GC	GC %	AT %	GC Skew	AT skew
Antipathes cf. *dichotoma*	19,969	5,153	3,715	4,584	6,468	8,300	41.7	58.3	0.099	−0.113
Bathypathes sp. 1	17,700	4,715	3,165	3,893	5,927	7,058	39.9	60.1	0.103	−0.114
Bathypathes n. sp. 2	17,700	4,717	3,166	3,892	5,925	7,058	39.9	60.1	0.103	−0.114
Bathypathes n. sp. 3	17,700	4,718	3,162	3,889	5,931	7,051	39.8	60.2	0.103	−0.114
Chrysopathes formosa NC008411	18,398	4,940	3,292	3,983	6,182	7,275	39.5	60.5	0.095	−0.112
Dendrobathypathes n. sp.	17,687	4,694	3,214	3,922	5,857	7,136	40.3	59.7	0.099	−0.110
Leiopathes cf. *glaberrima*	21,669	5,917	3,821	4,712	7,218	8,533	39.4	60.6	0.104	−0.099
Leiopathes expansa	21,653	5,913	3,819	4,711	7,210	8,530	39.4	60.6	0.105	−0.099
Leiopathes montana	21,672	5,888	3,777	4,677	7,160	8,454	39.3	60.7	0.106	−0.097
Myriopathes japonica NC027667	17,733	4,696	3,219	3,895	5,923	7,114	40.1	59.9	0.095	−0.116
Parantipathes cf. *hirondelle*	17,734	4,708	3,217	3,917	5,892	7,134	40.2	59.8	0.098	−0.112
Parantipathes hirondelle	17,734	4,709	3,216	3,917	5,892	7,133	40.2	59.8	0.098	−0.112
Parantipathes sp.	17,734	4,705	3,215	3,920	5,894	7,135	40.2	59.8	0.099	−0.112
Phanopathes sp.	20,304	5,542	3,481	4,404	6,877	7,885	38.8	61.2	0.117	−0.107
Sibopathes cf. *macrospina*	17,734	4,704	3,215	3,921	5,894	7,136	40.2	59.8	0.105	−0.112
Stauropathes cf. *punctata*	17,690	4,711	3,167	3,894	5,918	7,061	39.9	60.1	0.103	−0.114
Stauropathes arctica	17,700	4,716	3,165	3,892	5,927	7,057	39.9	60.1	0.103	−0.114
Stichopathes abyssicola	19,968	5,158	3,725	4,600	6,485	8,325	41.7	58.3	0.105	−0.114
Stichopathes luetkeni JX023266	20,448	5,927	3,137	4,069	7,315	7,206	35.2	64.8	0.129	−0.105
Stichopathes n. sp.	19,839	5,425	3,515	4,291	6,608	7,806	39.3	60.7	0.099	−0.098
Tanacetipathes thamnea MN265369	17,712	4,690	3,225	3,890	5,907	7,115	40.2	59.8	0.093	−0.115
Telopathes sp.	17,681	4,699	3,173	3,898	5,911	7,071	40	60	0.103	−0.114
Trissopathes cf. *tetracrada*	18,469	4,968	3,313	3,988	6,200	7,301	39.5	60.5	0.092	−0.110
Tylopathes n. sp.	17,679	4,603	3,334	3,944	5,797	7,278	41.2	58.8	0.084	−0.115

indel-free alignment is *ND4* spanning 1476 conserved bp (91.9% PI; 70.5% IS). Additional ML phylogenetic analysis of the *ND4* Gblock alignment recovered a tree with identical topology to the full mitochondrial tree, with high bootstrap nodal support for all major clades (>82% BS). A comparative *COX1* tree revealed weaker BS support values for all major clades (>57% BS). While *COX1* continues to be an effective marker for barcoding studies in Antipatharia (Brugler et al., 2013), future researchers may wish to consider the addition of *ND4* to further increase the resolving power of taxonomic identification.

Origins of Replication and Intergenic Regions

The origins of replication in mitogenomes are often associated with large intergenic spaces, inverted repeats, A+T rich regions and at the junction of conserved gene blocks (Pearson et al., 1996; Brugler and France, 2008; Hogan et al., 2019). Additionally, mitogenomes have two separate origins of replication (Clayton, 1992), one found on each strand; OriH found on the heavy strand and OriL found on the light strand. Brugler and France (2007) investigated the *ND2*-12S IGR as a possible location of OriH due to its large size. With only one complete antipatharian genome for their analysis, comparisons were made with other hexacoral species, and they ultimately rejected this location as the OriH. However, with the larger data set provided by the current study, we note abrupt compositional changes around this region, the presence of inverted repeats and relatively high conservation (aligning all *ND2*-12S IGRs produces a 278 bp region with 67.3% PI), all of which suggest the IGR *ND2*-12S is the most likely candidate for the OriH in Antipatharia.

Defining the exact location of OriL has proved difficult in invertebrates (Wolstenholme, 1992). Brugler and France (2008) proposed candidate regions between 12S-*CYTB* and trnM-16S for *Chrysopathes formosa* based on the abrupt changes in base composition at these locations. In the present study 12S-*CYTB* has a relatively balanced A+T/G+C base content (average 48.6% A+T) and a relatively small IGR (mean 86 bp). In contrast the IGRs trnM-16S and 16S-*COX3* both show an abrupt change in base composition and have a high A+T content (mean 65.4 and 64.5%, respectively), while IGR 16S-*COX3* has a relatively large IGR (mean 136 bp), making it the preferred candidate for OriL. Further investigation into the secondary structures of the IGRs, including presence of A+T stable stem loops, would be necessary to provide additional evidence for the location of OriH and OriL.

Open read frames of unknown function have not previously been reported for antipatharian mitogenomes. However, they are common in other hexacoral orders (Flot and Tillier, 2007; Emblem et al., 2014; Foox et al., 2015; Chi and Johansen, 2017). Their functionality in actinarians has been speculated to be that of transposon-like elements capable of influencing nearby genes, as possible enhancers or promotors (Zhang et al., 2017). Emblem et al. (2014) demonstrated that ORFs within

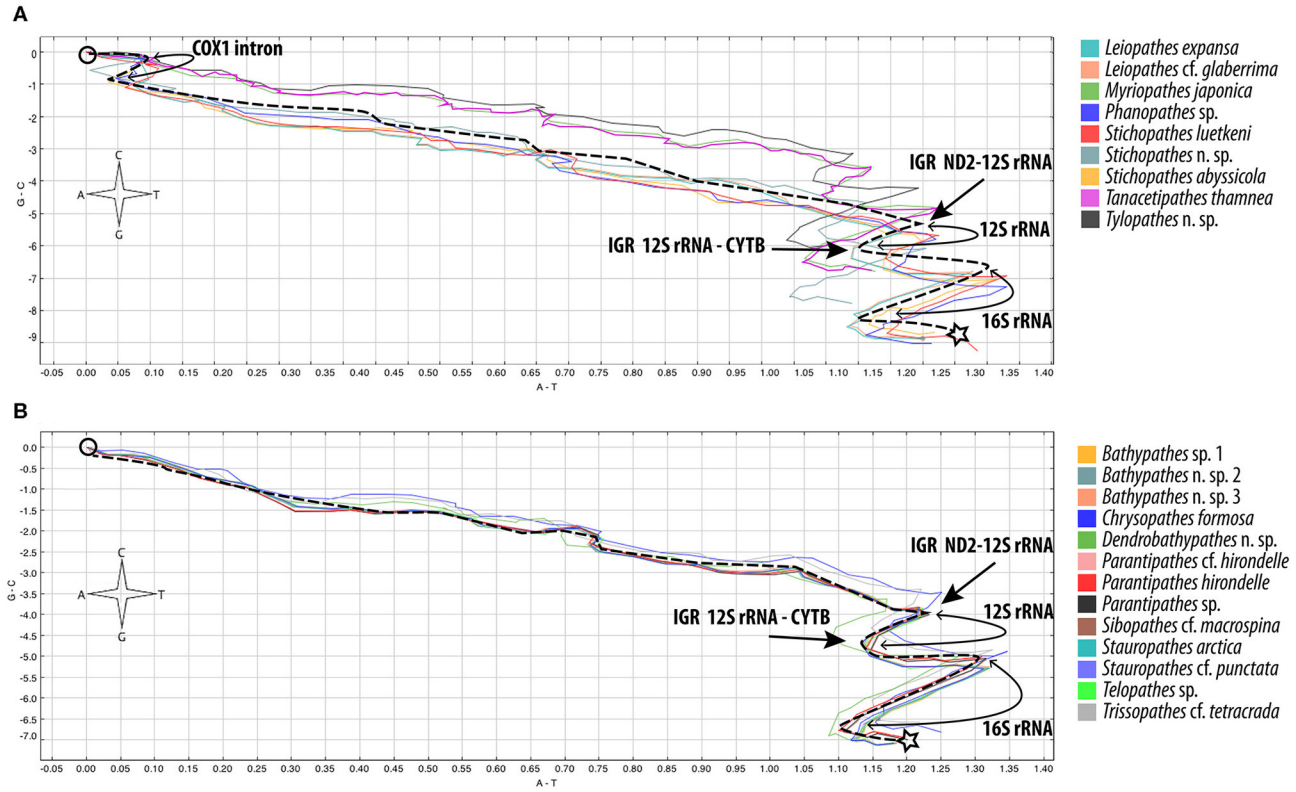

FIGURE 2 | DNA Walk [GraphDNA (Thomas et al., 2007)] results from vectorial representation of a linearized genome beginning at *COX1* (circular symbol) and ending at IGR *COX3-COX1* (star symbol). Each of the four nucleotides in the genome sequence is designated a direction as displayed on the compass. Units on axis are cumulative skew measured as number of nucleotides X 10^3 (Window size is displayed at 400 for ease of viewing). **(A)** Genomes with the *COX1* intron. **(B)** Genomes with the *COX1* intron absent. The dotted line represents the general shape of the walk. Abrupt changes in direction are characteristic of a separate evolutionary origin for that particular region.

actinarian mitogenomes are likely functional units. The lack of conserved ORFs across antipatharians suggests that many are likely to be small pseudogenes. However, small proteins, often defined as <100 amino acid residues (Su et al., 2013), have been shown to be responsible for important biological processes in other metazoans (Galindo et al., 2007). The largest ORF found in this study, 477 bp in *Phanopathes* sp. is the most likely candidate for a functional protein due to its size. Transposon-like elements have been demonstrated to play important roles in adaptation to environmental stress (Casacuberta and González, 2013). Considering the environmental extremes of antipatharian deep-sea habitats, the function of these ORFs may well be similar to transposon-like elements offering beneficial metabolic adaptations to the deep-sea.

The potential for non-homologous cross mapping of nuclear DNA of mitochondrial origin (nuMT) to mitochondrial DNA (mtDNA) assemblies [see Maude et al. (2019) for a discussion] was considered in light of the large number of varied ORFs found throughout the mitogenomes. BLAST analysis of the larger ORF (>70 bp) revealed no matches to hexacoral nuclear regions. Read coverage for ORF loci was consistent with coverage for the overall mitogenome (i.e., if similar copies were present in the nuclear genome, we might expect higher coverage). Additionally, we might expect higher sequence variability in these ORFs compared with other coding regions (e.g., greater disagreement of mapped reads in these ORFs), however this was not the case.

Introns

A cyclic evolutionary model of intron gain and loss has previously been proposed for the presence of the *COX1* intron in cnidarians (Goddard et al., 2006). Celis et al. (2017) suggest the *COX1* intron was inserted early in cnidarian history and rapidly invaded intron-less alleles via horizontal transfer due to the *HEG* gene. After becoming fixed in the population, it was subject to mutational degradation, losing *HEG* functionality, but continued to be inherited vertically as a *HEG* remnant. The effects of purifying selection resulted in the complete deletion of the intron and *HEG* from *COX1*. Support for this hypothesis in Antipatharia is evident in the variation of *HEG* sizes observed across families, with the presence of shorter *HEG* genes in Myriopathidae and Stylopathidae (657 bp) indicating they are in a later stage of the degradation period as compared to Antipathidae (1,062 bp), Aphanipathidae (981 bp) and Leiopathidae (996 bp). The absence of the *COX1* intron within the Cladopathidae and Schizopathidae

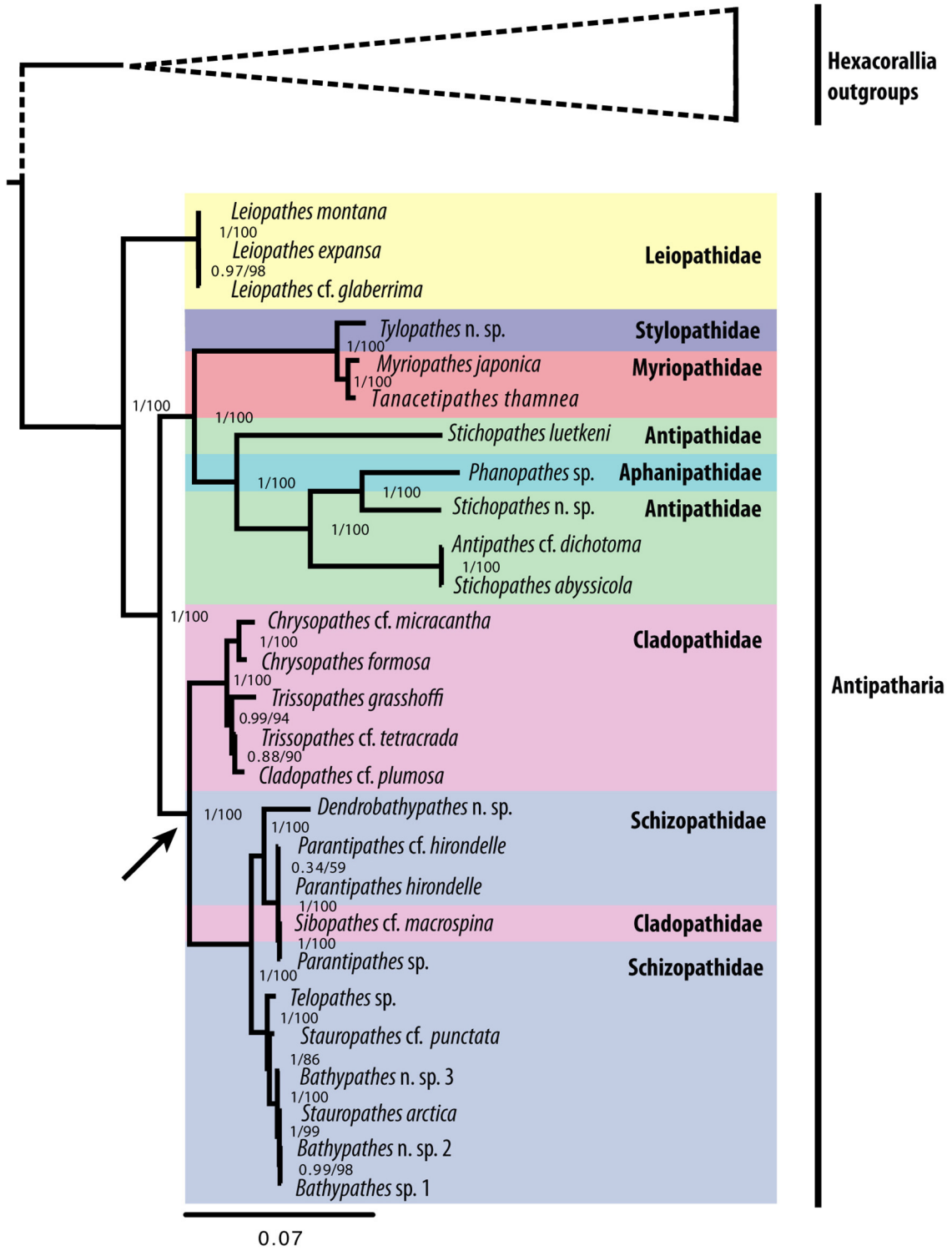

FIGURE 3 | Phylogenetic tree reconstruction based on all available (newly sequenced from this study and GenBank samples) antipatharian mitochondrial genomes using the 13 energy pathway genes based on a Bayesian inference (BI) and maximum likelihood (ML) analysis. The trees are rooted at a midpoint between Antipatharia and the hexacoral outgroups (See **Figure S1** for outgroup relationships). BI posterior probabilities and ML bootstrap values shown at nodes (BI/ML). The arrow indicates the apparent loss of the *COX1* intron at an internal node.

suggest a complete evolutionary cyclic history of intron invasion, degradation and deletion has occurred within antipatharians, as has previously been shown in Actinaria (Emblem et al., 2014), and in Scleractinia and Corallimorpharia (Celis et al., 2017). This is further implied by the phylogenetic analysis which suggests the *COX1* intron was present in the ancestral state due to its presence in Leiopathidae, which is sister to all other antipatharian families. It was then subject to a single loss in the branch leading to the Cladopathidae + Schizopathidae clade (see **Figure 3**), suggesting a close evolutionary relationship between these two families as shown by Brugler et al. (2013). Interestingly, species of Cladopathidae and Schizopathidae are the only antipatharians found in the abyssal zone >3,000 m (Molodtsova and Opresko, 2017). Whether the loss of the *COX1* intron is an adaptation to the deep-sea environment warrants further investigation.

In contrast to the *COX1* intron, the *ND5* intron is present within all sequenced genomes. The insertion position is at the same location as found in all hexacoral orders (Chi and Johansen, 2017), referred to as position 717 (Emblem et al., 2011). Emblem et al. (2011) propose that the *ND5* intron originally contained a *HEG* gene and was subject to horizonal transfer and a similar cyclic scenario as the *COX1* intron. However, at one stage, the insertion of *ND1* and *ND3* resulted in the intron becoming a compulsory element, resulting in a vertical pattern of inheritance, supported by the conserved intron position. In contrast, three insertion sites have been identified for the *COX1* intron across the hexacorals (Celis et al., 2017), suggesting a lack of positive selection.

Phylogenies and Interfamilial Relationships

Previous molecular studies show consistent congruent sister groupings between the following sets of antipatharian families: Cladopathidae + Schizopathidae (Brugler et al., 2013; Bo et al., 2018), Myriopathidae + Stylopathidae (Brugler et al., 2013), Antipathidae + Aphanipathidae (Lapian et al., 2007; Bo et al., 2009a, 2018; Lapian, 2009; Wagner et al., 2010; Brugler et al., 2013). The phylogenies presented in this study are in agreement with these family groupings. Based on morphology, Opresko (1998) considered Leiopathidae to be a distinctive family and suggested it may warrant a higher level classification, while Brugler et al. (2013) suggested it may be the most primitive family. However, molecular studies have shown conflicting results with both Antipathidae and Leiopathidae being recovered as sister to the remaining antipatharian families (Brugler et al., 2013; Bo et al., 2018). As the ingroup topology is sensitive to the choice of outgroup and number of outgroup samples (Smith, 1994), we have chosen to include three samples from a close sister order, Actiniaria, and a single representative from each of the three remaining hexacoral orders, Corallimorpharia, Scleractinia and Zoantharia. This study presents the largest molecular character set to date (13,255 characters) and supports Leiopathidae as sister to all other families, reconciling the morphological/molecular positions. This study should be considered a preliminary assessment of the interfamilial relationships within Antipatharia until broader geographic and taxonomic representation can be achieved using full mitogenomes.

The species reported here as *Sibopathes* cf. *macrospina* (family Cladopathidae) clustered within a clade with three *Parantipathes* species (family Schizopathidae) with marginal genetic differences. Similar results were reported by Brugler et al. (2013) for material from the Gulf of Mexico and Western Atlantic. This suggests *S.* cf. *macrospina* may indeed belong to the genus *Parantipathes*. There are a number of morphological differences reported between *S.* cf. *macrospina* and the type species of the genus *Sibopathes* [*S. gephura* van Pesch, 1914], that include pinnulation pattern, form of spines and morphology of polyps (van Pesch, 1914; Opresko, 1993; unpubl. observations T.M.). Molecular studies including *S. gephura* are necessary to validate the phylogenetic position of the genus *Sibopathes* and resolve the apparent polyphyly in Cladopathidae and Schizopathidae. In addition, species in the genera *Trissopathes* and *Cladopathes* formed a well-supported clade with *C.* cf. *plumosa* and *T.* cf. *tetracrada* in particular showing almost no evolutionary distance between them in the nuclear phylogenies (**Figures S4, S5**). Further studies may conclude that they represent the same genus, however it is significant to note that the mitogenomes of *C.* cf. *plumosa* and *T. grasshoffi* are currently incomplete.

Polyphyly in Antipathidae has been noted in previous studies (Brugler et al., 2013; Bo et al., 2018) with the suggestion that a taxonomic revision is necessary. In particular the genera *Antipathes* and *Stichopathes* have been posited for revision and splitting (Bo et al., 2012a, 2018). The present study found the single *Antipathes* sample *A.* cf. *dichotoma,* formed a 100% BS (BPP=1) supported clade with *S. abyssicola,* with little evolutionary distance between them. A similar lack of phylogenetic signal between the genera *Antipathes* and *Stichopathes* has been reported by previous studies (Bo et al., 2012a, 2018; Brugler et al., 2013). Bo et al. (2012a) highlights that the single-stem morphology (attributed to *Stichopathes*-like specimens), is an unreliable characteristic as it may have evolved independently in different taxa. This would account for the lack of grouping between the three *Stichopathes* species in this study.

With the current study, only one sample is representative of Aphanipathidae, *Phanopathes* sp., which forms a well-supported clade with the antipathid, *Stichopathes* n. sp.. This is consistent with the findings of previous studies (Brugler et al., 2013; Bo et al., 2018), which have found *Phanopathes* species clustering with *A. dichotoma* and various *Stichopathes* species. With only one full genome representing Aphanipathidae, the current analysis is limited in scope, however the high support values for the *Phanopathes* sp. + *Stichopathes* n. sp. clade is noteworthy, although the large branch lengths indicate high genetic differentiation between these species. Bo et al. (2018) suggests that the name bearing type for the genus *Antipathes* and ultimately the family Antipathidae, *A. dichotoma* Pallas, 1766, is likely to be unrepresentative of the genus and therefore the family. Our study supports the need for taxonomic revision within Antipathidae and Aphanipathidae (Brugler et al., 2013; Bo et al., 2018), which would benefit from further sequencing of full mitogenomes representative of a greater range of diversity within these families.

The polyphyly and particularly short genetic distances found within two genera of the Schizopathidae samples; *Bathypathes* and *Stauropathes*, support the morphological similarities observed between *Telopathes*, *Stauropathes* and *Bathypathes* (MacIsaac et al., 2013). They form a tight clade in the current and previous studies (MacIsaac et al., 2013; Bo et al., 2018), warranting further morphological analysis to validate these genera.

Conclusions and Future Investigations

Antipatharia appears to have a stable gene order and content, with the exception of the absence of the *COX1* intron in two families. The most variable gene region is found to be *ND4,* in contrast to the commonly recommended *COX1* 'barcode of life'. The variability in size range of IGRs, presence of multiple ORFs and *HEG* gene length variations across families, offer an avenue for future studies to investigate additional evolutionary scenarios and possible adaptations to metabolic functions. Phylogenetically we find that Leiopathidae is sister to all other antipatharian families. Families Antipathidae, Cladopathidae and Schizopathidae are polyphyletic, and several genera may be in need of taxonomic revision.

DATA AVAILABILITY STATEMENT

The datasets presented in this study can be found in online repositories. The names of the repository/repositories and accession number(s) can be found in the article/**Supplementary Material**.

AUTHOR CONTRIBUTIONS

The project was conceived by AA, RH, and CY and designed by CY with input from NB. Sample collection, initial taxonomic identification, and DNA extraction was carried out by AA and RH, with the exception of *Sibopathes* cf. *macrospina*, which was collected by AW. Final taxonomic identification was carried out by TM. DNA library preparation for sequencing was carried out by KH and NB. The pipeline assembly including data cleaning, genome assembly, annotation, and all downstream analysis was carried out by NB with advice from CY. The manuscript was written by NB with contributions from all authors. All authors edited the manuscript before submission.

FUNDING

Research surveys from 2013 to 2016 were supported by the Marine Institute and funded under the Marine Research Programme by the Irish Government. Research Survey CE15009 contributes to outputs of the Irish Center for Research in Applied Geosciences funded through Science Foundation Ireland Grant Number 13/RC/2092 and co-funded under the European Regional Development Fund 2014–2020. Research Survey CE17008 was conducted as part of the project Exploiting and conserving deep-sea genetic resources funded by Science Foundation Ireland and the Marine Institute under the Investigators Programme Grant No. SFI/15/1A/3100 and co-funded under the European Regional Development Fund 2014-2020. RH was supported by Brazilian National Council for Scientific and Technological Development (CNPq) Grant No. 248444/2013-1. TM was funded by RF State Assignment (0149-2019-0009).

ACKNOWLEDGMENTS

Samples were collected using ROV Holland I deployed from RV Celtic Explorer with support from the officers, crew and ROV technical team. NB and CY would like to thank Nadia Santodomingo for her support and advice.

SUPPLEMENTARY MATERIAL

The Supplementary Material for this article can be found online at: https://www.frontiersin.org/articles/10.3389/fmars.2020.00440/full#supplementary-material

REFERENCES

Al-Lihaibi, S. S., Ayyad, S.-E. N., Shaher, F., and Alarif, W. M. (2010). Antibacterial sphingolipid and steroids from the black coral *Antipathes dichotoma*. *Chem. Pharm. Bull.* 58, 1635–1638. doi: 10.1248/cpb.58.1635

Andrews, S. (2010). *FastQC: A Quality Control Tool for High Throughput Sequence Data*. Available online at: http://www.bioinformatics.babraham.ac.uk/projects/fastqc (accessed August, 2019).

Benson, G. (1999). Tandem repeats finder: a program to analyze DNA sequences. *Nucleic Acids Res.* 27, 573–580. doi: 10.1093/nar/27.2.573

Bernt, M., Donath, A., Jühling, F., Externbrink, F., Florentz, C., Fritzsch, G., et al. (2013). MITOS: Improved *de novo* metazoan mitochondrial genome annotation. *Mol. Phylogenet. Evol.* 69, 313–319. doi: 10.1016/j.ympev.2012.08.023

Bininda-Emonds, O. R. P. (2005). *seqCat.pl*. Available online at: http://users-cs.au.dk/kmt/scriptlist/seqCat.txt (accessed March, 2020).

Bo, M., Barucca, M., Biscotti, M. A., Brugler, M. R., Canapa, A., Canese, S., et al. (2018). Phylogenetic relationships of mediterranean black corals (*Cnidaria: Anthozoa: Hexacorallia*) and implications for classification within the order *Antipatharia*. *Invertebr. Syst.* 32, 1102–1110. doi: 10.1071/IS17043

Bo, M., Barucca, M., Biscotti, M. A., Canapa, A., Lapian, H. F. N., Olmo, E., et al. (2009a). Description of *Pseudocirrhipathes* (*Cnidaria: Anthozoa: Hexacorallia: Antipathidae*), a new genus of whip black corals from the Indo-Pacific. *Ital. J. Zool.* 76, 392–402. doi: 10.1080/11250000802684104

Bo, M., Bavestrello, G., Barucca, M., Makapedua, D. M., Poliseno, A., Forconi, M., et al. (2012a). Morphological and molecular characterization of the problematic whip black coral genus stichopathes (*Hexacorallia: Antipatharia*) from indonesia (north sulawesi, celebes sea). *Zool. J. Linn. Soc.* 166, 1–13. doi: 10.1111/j.1096-3642.2012.00834.x

Bo, M., Bavestrello, G., Canese, S., Giusti, M., Salvati, E., Angiolillo, M., et al. (2009b). Characteristics of a black coral meadow in the twilight zone of the central mediterranean sea. *Mar. Ecol. Progr. Ser.* 397, 53–61. doi: 10.3354/meps08185

Bo, M., Bavestrello, G., Kurek, D., Paasch, S., Brunner, E., Born, R., et al. (2012b). Isolation and identification of chitin in the black coral parantipathes larix (*Anthozoa: Cnidaria*). *Int. J. Biol. Macromol.* 51, 129–137. doi: 10.1016/j.ijbiomac.2012.04.016

Boore, J. L. (2006). The use of genome-level characters for phylogenetic reconstruction. *Trends Ecol. Evol.* 21, 439–446. doi: 10.1016/j.tree.2006.05.009

Boore, J. L., and Fuerstenberg, S. I. (2008). Beyond linear sequence comparisons: the use of genome-level characters for phylogenetic reconstruction. *Philos. Trans. R. Soc. B Biol. Sci.* 363, 1445–1451. doi: 10.1098/rstb.2007.2234

Bouckaert, R., Heled, J., Kühnert, D., Vaughan, T., Wu, C. H., Xie, D., et al. (2014). BEAST 2: a software platform for bayesian evolutionary analysis. *PLoS Comput. Biol.* 10:e1003537. doi: 10.1371/journal.pcbi.1003537

Brockman, S. A., and McFadden, C. S. (2012). The mitochondrial genome of *Paraminabea aldersladei* (*Cnidaria: Anthozoa: Octocorallia*) supports intramolecular recombination as the primary mechanism of gene rearrangement in octocoral mitochondrial genomes. *Genome Biol. Evol.* 4, 994–1006. doi: 10.1093/gbe/evs074

Brugler, M., Opresko, D. M., and France, S. C. (2013). The evolutionary history of the order *Antipatharia* (*Cnidaria : Anthozoa : Hexacorallia*) as inferred from mitochondrial and nuclear DNA : implications for black coral taxonomy and systematics. *Zool. J. Linn. Soc.* 169, 312–361. doi: 10.1111/zoj.12060

Brugler, M. R., and France, S. C. (2007). The complete mitochondrial genome of the black coral *Chrysopathes formosa* (*Cnidaria : Anthozoa : Antipatharia*) supports classification of antipatharians within the subclass *Hexacorallia. Mol. Phylogenetics Evol.* 42, 776–788. doi: 10.1016/j.ympev.2006.08.016

Brugler, M. R., and France, S. C. (2008). The mitochondrial genome of a deep-sea bamboo coral (*Cnidaria, Anthozoa, Octocorallia, Isididae*): genome structure and putative origins of replication are not conserved among octocorals. *J. Mol. Evol.* 67, 125–136. doi: 10.1007/s00239-008-9116-2

Cairns, S. D. (2007). Deep-water corals: an overview with special reference to diversity and distribution of deep-water scleractinian corals. *Bull. Mar. Sci.* 81, 311–322. Available online at: https://repository.si.edu/handle/10088/7536

Casacuberta, E., and González, J. (2013). The impact of transposable elements in environmental adaptation. *Mol. Ecol.* 22, 1503–1517. doi: 10.1111/mec.12170

Castresana, J. (2000). Selection of conserved blocks from multiple alignments for their use in phylogenetic analysis. *Mol. Biol. Evol.* 17, 540–552. doi: 10.1093/oxfordjournals.molbev.a026334

Celis, J. S., Edgell, D. R., Stelbrink, B., Wibberg, D., Hauffe, T., Blom, J., et al. (2017). Evolutionary and biogeographical implications of degraded LAGLIDADG endonuclease functionality and group i intron occurrence in stony corals (*Scleractinia*) and mushroom corals (*Corallimorpharia*). *PLoS ONE* 12:e0173734. doi: 10.1371/journal.pone.0173734

Chi, S. I., and Johansen, S. D. (2017). Zoantharian mitochondrial genomes contain unique complex group I introns and highly conserved intergenic regions. *Gene* 628, 24–31. doi: 10.1016/j.gene.2017.07.023

Clayton, D. A. (1992). Transcription and replication of mitochondrial DNA. *Hum. Reprod.* 15, 11–17. doi: 10.1093/humrep/15.suppl_2.11

Crampton-Platt, A., Yu, D. W., Zhou, X., and Vogler, A. P. (2016). Mitochondrial metagenomics : letting the genes out of the bottle. *Gigascience* 5:15. doi: 10.1186/s13742-016-0120-y

Darriba, D., Taboada, G. L., Doallo, R., and Posada, D. (2012). jModelTest 2: more models, new heuristics and parallel computing. *Nat. Methods* 9:772. doi: 10.1038/nmeth.2109

Ehrlich, H. (2010). *Biological Materials of Marine Origin. Invertebrates*. Dordrecht: Springer-Verlag, 569. doi: 10.1007/978-94-007-5730-1

Emblem, Å., Karlsen, B. O., Evertsen, J., and Johansen, S. D. (2011). Mitogenome rearrangement in the cold-water scleractinian coral *Lophelia pertusa* (*Cnidaria, Anthozoa*) involves a long-term evolving group I intron. *Mol. Phylogenet. Evol.* 61, 495–503. doi: 10.1016/j.ympev.2011.07.012

Emblem, Å., Okkenhaug, S., Weiss, E. S., Denver, D. R., Karlsen, B. O., Moum, T., et al. (2014). Sea anemones possess dynamic mitogenome structures. *Mol. Phylogenet. Evol.* 75, 184–193. doi: 10.1016/j.ympev,.2014.02.016

Falkenberg, M., Larsson, N.-G., and Gustafsson, C. M. (2007). DNA replication and transcription in mammalian mitochondria. *Annu. Rev. Biochem.* 76, 679–699. doi: 10.1146/annurev.biochem.76.060305.152028

Figueroa, D. F., and Baco, A. R. (2014). Octocoral mitochondrial genomes provide insights into the phylogenetic history of gene order rearrangements, order reversals, and cnidarian phylogenetics. *Genome Biol. Evol.* 7, 391–409. doi: 10.1093/gbe/evu286

Figueroa, D. F., Hicks, D., and Figueroa, N. J. (2019). The complete mitochondrial genome of *Tanacetipathes thamnea* Warner, 1981 (*Antipatharia: Myriopathidae*). *Mitochondrial DNA Part B Resour.* 4, 4109–4110. doi: 10.1080/23802359.2019.1692701

Flot, J. F., and Tillier, S. (2007). The mitochondrial genome of *Pocillopora* (*Cnidaria: Scleractinia*) contains two variable regions: the putative D-loop and a novel ORF of unknown function. *Gene* 401, 80–87. doi: 10.1016/j.gene.2007.07.006

Foox, J., Brugler, M., Siddall, M. E., and Rodríguez, E. (2015). Multiplexed pyrosequencing of nine sea anemone (*Cnidaria: Anthozoa: Hexacorallia: Actiniaria*) mitochondrial genomes. *Mitochondrial DNA* 27, 2826–2832. doi: 10.3109/19401736.2015.1053114

Galindo, M. I., Pueyo, J. I., Fouix, S., Bishop, S. A., and Couso, J. P. (2007). Peptides encoded by short ORFs control development and define a new eukaryotic gene family. *PLOS Biol.* 5:e106. doi: 10.1371/journal.pbio.0050106

Ghandourah, M. A., and Alorfi, H. S. (2019). New cytotoxic fatty acid esters from the black coral, *Antipathes dichotoma*. *Trop. J. Pharm. Res.* 18, 69–74. doi: 10.4314/tjpr.v18i1.11

Goddard, M. R., Leigh, J., Roger, A. J., and Pemberton, A. J. (2006). Invasion and persistence of a selfish gene in the Cnidaria. *PLoS ONE* 1:e3. doi: 10.1371/journal.pone.0000003

Greiner, S., Lehwark, P., and Bock, R. (2019). OrganellarGenomeDRAW (OGDRAW) version 1.3.1: expanded toolkit for the graphical visualization of organellar genomes. *Nucleic. Acids Res.* 47, W59–W64. doi: 10.1093/nar/gkz238

Guindon, S., and Gascuel, O. (2003). A simple, fast, and accurate algorithm to estimate large phylogenies by maximum likelihood. *Syst. Biol.* 52, 696–704. doi: 10.1080/10635150390235520

Hahn, C., Bachmann, L., and Chevreux, B. (2013). Reconstructing mitochondrial genomes directly from genomic next-generation sequencing reads—a baiting and iterative mapping approach. *Nucleic Acids Res.* 41:e129. doi: 10.1093/nar/gkt371

Hebert, P. D. N., Cywinska, A., Ball, S. L., and DeWaard, J. R. (2003). Biological identifications through DNA barcodes. *Proc. R. Soc. B Biol. Sci.* 270, 313–321. doi: 10.1098/rspb.2002.2218

Hellberg, M. E. (2006). No variation and low synonymous substitution rates in coral mtDNA despite high nuclear variation. *BMC Evol. Biol.* 6:24. doi: 10.1186/1471-2148-6-24

Hoang, D. T., Chernomor, O., von Haeseler, A., Minh, B. Q., and Vinh, L. S. (2017). UFBoot2: improving the ultrafast bootstrap approximation. *Mol. Biol. Evol.* 35, 518–522. doi: 10.1093/molbev/msx281

Hogan, R. I., Hopkins, K., Wheeler, A. J., Allcock, A. L., and Yesson, C. (2019). Novel diversity in mitochondrial genomes of deep-sea *Pennatulacea* (*Cnidaria: Anthozoa: Octocorallia*). *Mitochondrial DNA A* 30, 764–777. doi: 10.1080/24701394.2019.1634699

Kalyaanamoorthy, S., Minh, B. Q., Wong, T. K. F., von Haeseler, A., and Jermiin, L. S. (2017). ModelFinder: fast model selection for accurate phylogenetic estimates. *Nat. Methods* 14:587. doi: 10.1038/nmeth.4285

Katoh, K., and Standley, D. M. (2013). MAFFT Multiple sequence alignment software version 7: improvements in performance and usability. *Mol. Biol. Evol.* 30, 772–780. doi: 10.1093/molbev/mst010

Kayal, E., Roure, B., Philippe, H., Collins, A. G., and Lavrov, D. V. (2013). Cnidarian phylogenetic relationships as revealed by mitogenomics. *BMC Evol. Biol.* 13:5. doi: 10.1186/1471-2148-13-5

Kearse, M., Moir, R., Wilson, A., Stones-Havas, S., Cheung, M., Sturrock, S., et al. (2012). Geneious Basic: an integrated and extendable desktop software platform for the organization and analysis of sequence data. *Bioinformatics* 28, 1647–1649. doi: 10.1093/bioinformatics/bts199

Lapian, H. F. N. (2009). Biodiversity study of black coral (Order: *Antipatharia*) collected from Manado, Indonesia based on rDNA internal transcribed spacer (ITS) sequences analysis. *Biodiversitas J. Biol. Divers.* 10, 1–5. doi: 10.13057/biodiv/d100101

Lapian, H. F. N., Barucca, M., Maria, B., Marzia, A. B., Canapa, A., Tazioli, S., et al. (2007). A systematic study of some black corals species (*Antipatharia, Hexacorallia*) based on rDNA internal transcribed spacers sequences. *Mar. Biol.* 151, 785–792. doi: 10.1007/s00227-006-0525-8

Lin, M. F., Kitahara, M. V., Luo, H., Tracey, D., Geller, J., Fukami, H., et al. (2014). Mitochondrial genome rearrangements in the scleractinia/corallimorpharia complex: implications for coral phylogeny. *Genome Biol. Evol.* 6, 1086–1095. doi: 10.1093/gbe/evu084

Lobry, J. R. (1996). A simple vectorial representation of DNA sequences for the detection of replication origins in bacteria. *Biochimie* 78, 323–326. doi: 10.1016/0300-9084(96)84764-X

Love, M. S., Yoklavich, M. M., Black, B. A., and Andrews, A. H. (2007). Age of black coral (*Antipathes dendrochristos*) colonies, with notes on associated invertebrate species. *Bull. Mar. Sci.* 80, 391–399. Available online at: https://www.ingentaconnect.com/contentone/umrsmas/bullmar/2007/00000080/00000002/art00008

Lowe, T. M., and Chan, P. P. (2016). tRNAscan-SE On-line: integrating search and context for analysis of transfer RNA genes. *Nucleic Acids Res.* 44, W54–W57. doi: 10.1093/nar/gkw413

MacIsaac, K. G., Anstey, L. J., Best, M., Kenchington, E. L., Brugler, M. R., and Jordan, T. (2013). Telopathes magna gen. nov., spec. nov. (*Cnidaria: Anthozoa: Antipatharia: Schizopathidae*) from deep waters off Atlantic Canada and the first molecular phylogeny of the deep-sea family schizopathidae. *Zootaxa*. 3700, 237–258. doi: 10.11646/zootaxa.3700.2.3

Martin, M. (2011). Cutadapt removes adapter sequences from high-throughput sequencing reads. *EMBnet* 17, 10–12. doi: 10.14806/ej.17.1.200

Maude, H., Davidson, M., Charitakis, N., Diaz, L., Bowers, W. H. T., Gradovich, E., et al. (2019). NUMT confounding biases mitochondrial heteroplasmy calls in favor of the reference allele. *Front. Cell Dev. Biol.* 7:201. doi: 10.3389/fcell.2019.00201

Medina, M., Collins, A. G., Takaoka, T. L., Kuehl, J. V., and Boore, J. L. (2006). Naked corals: skeleton loss in *Scleractinia*. *Proc. Natl. Acad. Sci. U S A.* 103, 9096–9100. doi: 10.1073/pnas.0602444103

Miller, M. A., Pfeiffer, W., and Schwartz, T. (2010). Creating the CIPRES science gateway for inference of large phylogenetic trees. *Proc. Gatew. Comput. Environ. Work.* 89, 1–8. doi: 10.1109/GCE.2010.5676129

Molodtsova, T., and Opresko, D. (2020). *World List of Antipatharia. Antipatharia*. Accessed through: world register of marine species Available Online at: http://www.marinespecies.org/aphia.php?p=taxdetails&id=22549 (accessed 05 January 2020).

Molodtsova, T. N., and Opresko, D. M. (2017). Black corals (*Anthozoa: Antipatharia*) of the clarion-clipperton fracture zone. *Mar. Biodivers.* 47, 349–365. doi: 10.1007/s12526-017-0659-6

Nguyen, L.-T., Schmidt, H. A., von Haeseler, A., and Minh, B. Q. (2014). IQ-TREE: A fast and effective stochastic algorithm for estimating maximum-likelihood phylogenies. *Mol. Biol. Evol.* 32, 268–274. doi: 10.1093/molbev/msu300

Opresko, D. M. (1993). A new species of sibopathes (*Cnidaria: Anthozoa: Antipatharia: Antipathidae*) from the gulf of Mexico. *Proc. Biol. Soc. Washington.* 106, 195–203.

Opresko, D. M. (1998). Three new species of *Leiopathes* (*Cnidaria: Anthozoa: Antipatharia*) from southern Australia. *Rec. South Aust. Museum* 31, 99–111. Available Online at: https://www.biodiversitylibrary.org/part/78875 (accessed March, 2020).

Pearson, C. E., Zorbas, H., Price, G. B., and Zannis-Hadjopoulos, M. (1996). Inverted repeats, stem-loops, and cruciforms: significance for initiation of DNA replication. *J. Cell. Biochem.* 63, 1–22. doi: 10.1002/(SICI)1097-4644(199610)63:1<1::AID-JCB1>3.0.CO;2-3

Perna, N. T., and Kocher, T. D. (1995). Patterns of nucleotide composition at fourfold degenerate sites of animal mitochondrial genomes. *J. Mol. Evol.* 41, 353–358. doi: 10.1007/BF00186547

Poliseno, A., Santos, M. E. A., Kise, H., Macdonald, B., Quattrini, A. M., McFadden, C. S., et al. (2020). Evolutionary implications of analyses of complete mitochondrial genomes across order Zoantharia (Cnidaria: Hexacorallia). *J. Zool. Syst. Evol. Res.* 1–11. doi: 10.1111/jzs.12380

Qi, S.-H., Su, G.-C., Wang, Y.-F., Liu, Q.-Y., and Gao, C.-H. (2009). Alkaloids from the South China Sea black coral *Antipathes dichotoma*. *Chem. Pharm. Bull.* 57, 87–88. doi: 10.1248/cpb.57.87

Rambaut, A., Drummond, A. J., Xie, D., Baele, G., and Suchard, M. A. (2018). Posterior summarization in bayesian phylogenetics using Tracer 1.7. *Syst. Biol.* 67, 901–904. doi: 10.1093/sysbio/syy032

Rice, P., Longden, L., and Bleasby, A. (2000). EMBOSS: The European molecular biology open software suite. *Trends Genet.* 16, 276–277. doi: 10.1016/S0168-9525(00)02024-2

Roberts, J. M., Wheeler, A. J., Freiwald, A., and Cairns, S. (2009). *Cold-Water Corals: The Biology and Geology of Deep-Sea Coral Habitats*. Cambridge: Cambridge University Press, 334. doi: 10.1017/CBO9780511581588

Ronquist, F., Teslenko, M., Van Der Mark, P., Ayres, D. L., Darling, A., Höhna, S., et al. (2012). Mrbayes 3.2: efficient bayesian phylogenetic inference and model choice across a large model space. *Syst. Biol.* 61, 539–542. doi: 10.1093/sysbio/sys029

Shimodaira, H. (2002). An approximately unbiased test of phylogenetic tree selection. *Syst. Biol.* 51, 492–508. doi: 10.1080/10635150290069913

Sinniger, F., Chevaldonn,é, P., and Pawlowski, J. (2007). Mitochondrial genome of *Savalia savaglia* (*Cnidaria, Hexacorallia*) and early metazoan phylogeny. *J. Mol. Evol.* 64, 196–203. doi: 10.1007/s00239-006-0015-0

Sinniger, F., and Pawloski, J. (2009). The partial mitochondrial genome of *Leiopathes glaberrima* (*Hexacorallia: Antipatharia*) and the first report of the presence of an intron in COI in black corals. *Galaxea, J. Coral Reef Stud.* 11, 21–26. doi: 10.3755/galaxea.11.21

Smith, A. B. (1994). Rooting molecular trees: problems and strategies. *Biol. J. Linn. Soc.* 51, 279–292. doi: 10.1111/j.1095-8312.1994.tb00962.x

Su, M., Ling, Y., Yu, J., Wu, J., and Xiao, J. (2013). Small proteins: untapped area of potential biological importance. *Front. Genet.* 4:286. doi: 10.3389/fgene.2013.00286

Thomas, J. M., Horspool, D., Brown, G., Tcherepanov, V., and Upton, C. (2007). GraphDNA: a java program for graphical display of DNA composition analyses. *BMC Bioinformatics* 8:21. doi: 10.1186/1471-2105-8-21

van Pesch, A. J. (1914). The antipatharia of the siboga expedition. *Siboga-Expeditie Monographe* 17, 1–258.

Wagner, D., Brugler, M. R., Opresko, D. M., France, S. C., Montgomery, A. D., and Toonen, R. J. (2010). Using morphometrics, in situ observations and genetic characters to distinguish among commercially valuable Hawaiian black coral species. *Invertebr. Syst.* 24, 271–290. doi: 10.1071/IS10004

Wagner, D., Luck, D. G., and Toonen, R. J. (2012). The biology and ecology of black corals (*Cnidaria: Anthozoa: Hexacorallia: Antipatharia*). *Adv. Mar. Biol.* 63, 67–132. doi: 10.1016/B978-0-12-394282-1.00002-8

Wolstenholme, D. R. (1992). Animal mitochondrial DNA: structure and evolution. *Int. Rev. Cytol.* 141, 173–216. doi: 10.1016/S0074-7696(08)62066-5

Zhang, B., Zhang, Y. H., Wang, X., Zhang, H. X., and Lin, Q. (2017). The mitochondrial genome of a sea anemone *Bolocera* sp. exhibits novel genetic structures potentially involved in adaptation to the deep-sea environment. *Ecol. Evol.* 7, 4951–4962. doi: 10.1002/ece3.3067

Conflict of Interest: The authors declare that the research was conducted in the absence of any commercial or financial relationships that could be construed as a potential conflict of interest.